SESSION IV

LMFBR ACCIDENT ANALYSIS

Tuesday, August 29, 1972
CHAIRMAN: M. Silberberg

CHAIRMAN'S OPENING REMARKS

Today I am pinch hitting for Harry Morewitz, of A.I., who was listed on the program but was unable to be with us at the conference. The subject for the first session this morning is entitled "LMFBR Accident Analysis." Although there are only two papers in the session I believe they will each satisfy quite well some of the objectives outlined for the Conference yesterday by Dr. Moeller, namely, to update specific technology in terms of need and application. One paper deals with the approach and basis for setting system design requirements, or for making design decisions in the LMFBR. The other paper describes a test program related to the solution of an air cleaning design problem associated with a specific sodium accident consideration.

ACCIDENT ANALYSIS FOR LMFBR ENGINEERED SAFEGUARDS DESIGN*

M. Silberberg
R. Koontz
L. Baurmash
R. P. Johnson
Atomics International
A Division of North American Rockwell Corporation
Canoga Park, California

Abstract

The release and control of radioactive material which becomes airborne as a result of the Hypothetical Core Disruptive Accident (HCDA) and sodium fires can be properly evaluated by a system of Codes (SOFAACS) developed for the Liquid Metal Fast Breeder Reactor (LMFBR) by Atomics International. These codes, and the applications of their use for LMFBR safety analysis and engineered safeguards design, are summarized. The codes include SOFIRE II, HAA-3, and SODROP models, which compute, respectively, sodium burning rate and heat transfer from open pool fires, burning and heat transfer controlled by convection through openings in partitions, behavior of the sodium oxide, fuel, and fission product aerosols, including agglomeration and settling, and sodium burning and energy release rates from sodium dispersed into inerted cells or air containment.

Use of these codes, in conjunction with required data from model experiments and scaling considerations, allows a realistic assessment of: (1) the design bases and requirements for engineered safeguards for meeting reactor siting criteria, and (2) the need for air cleaning systems during sodium fires for reducing postaccident cleanup.

I. Introduction

Experimental information and analytical models which describe the characteristics of energy release from sodium fires and the transport of sodium oxide, fuel, and fission product aerosols, under postulated Liquid Metal Fast Breeder Reactor (LMFBR) accident conditions, have been under development at Atomics International (AI) for the USAEC. The models which have been developed are being utilized in the evaluation of the design requirements for LMFBR containment systems.

Specific aspects of these studies have been described at previous Air Cleaning Conferences,[1-4] as they progressed through various phases of the program. The purpose of this paper is to summarize the functional relationships and key features of the various analytical models, and their wide application to accident analysis in several areas of LMFBR engineered safeguards design. The paper does not provide a detailed description of these models, but it is intended to provide sufficient information to inform the plant safeguards systems designer of a

*Work performed under USAEC Contract AT(04-3)-824

sound basis and systematic approach to the development of design requirements information. The availability of this systems design tool eliminates the use of first-order approximations and similar approaches which may lead to improper decisions in the systems design process (e.g., unrealistic, upper-limit design conservatism vs optimistic design with nonconservative margins).

The development of the analytical methods for treating sodium fires consequences and aerosol transport behavior for postulated LMFBR accidents have proceeded in parallel, and generally have been reported and discussed previously, as independent technology areas. In contrast with previous efforts, the material summarized here places particular emphasis on identifying the functional interfaces between sodium fires and aerosol transport in the application of the various models to accident analyses which may determine the basis for engineered safeguards design.

II. Sodium Fire and Aerosol Accident Analysis Codes System

AI has developed for the USAEC, under the LMFBR Safety Program, a series of heat - mass transfer and aerosol models which allow computation of the source terms and containment design leak rates produced by a variety of postulated LMFBR accidents. These models have been programmed into several codes which, when properly interfaced, allow one to follow the course of the accident consequences in terms of data for containment design and/or site radiological dose. Depending on the application, one can compute the leakage of radioactive materials for various assumed design leak rates, based on the mass of material (sodium, fuel, or fission products) and the pressure generated at any location in the containment system. Ventilation and gas recirculation system design requirements for cooling, pressure reduction, air cleaning, or deposition can also be computed.

The individual codes, their applications, and functions are briefly presented. The total system for these codes is designated SOFAACS.

A. SOFIRE II (Sodium Pool Fires and Spills)

The design pressure of the outer containment buildings in the LMFBR is currently based upon a large sodium pool fire in a primary heat transfer system equipment cell (below the operating floor) which is open, via an equipment access port, during maintenance. The two-cell version of the sodium pool burning code, SOFIRE II,[5] was developed to compute the restricted heat and mass transfer between cell and building, for determining pressure rise. Experimental verification of SOFIRE II (2-cell) is currently underway, to verify its adequacy for design, and, if required, to provide information for appropriate modification. The major item in the model requiring verification is the oxygen transfer rate from the building to the cell. A single, closed cell version of SOFIRE II is also available for predicting the consequences of large spills in primary system cells. The characteristics of SOFIRE II, in terms of functions, input requirements, and design data output, are listed in Table 1.

TABLE 1

SOFIRE II CHARACTERISTICS

1-Cell Code

Functions	Input Requirements	Design Data Output
Sodium Pool, Gas, and Wall Heat Transfer Rates	Peroxide-Monoxide Ratio, 0 to 1	Primary Cell Design Pressure
Sodium Pool Fire Burning Rates		Source of Aerosol for HAA-3
Pool, Gas, and Wall Temperatures		Cell Liner Temperature
		Concrete Temperature
Oxygen Consumption (initial oxygen from 0 to 21%)		Oxygen Consumed
Cell Pressure Rise		Sodium Burned
Sodium Consumption		

2-Cell Code

Functions	Input Requirements	Design Data Output
Sodium Pool, Gas, and Wall Heat Transfer Rates	Peroxide-Monoxide Ratio, 0 to 1	Source of Aerosol for HAA-3
Sodium Pool Fire Burning Rates		Cell Design Pressure Rise
Restricted Opening Mass Transfer		Ventilation Requirements (if low-pressure containment)
Oxygen Consumption (initial oxygen from 1 to 21%)		Oxygen Consumed
Pool, Gas, and Wall Temperatures		Sodium Burned and Remaining
Pressure (net), Primary Cell and Building		

B. SODROP (Dispersed Sodium Fires)

Design pressure considerations for the primary heat transfer system cells in the LMFBR may include the pressure rise computed from the energy transferred to the gas from hot sodium coolant released in dispersed form into the cell following a postulated pipe rupture accident. Previous upper-limit calculations have involved complete reaction of all oxygen in the inert gas (1 to 2% O_2) cell atmosphere with sodium and/or efficient mixing of cell gas with hot, relatively small particles of sodium spray. Calculational models are now under development, in conjunction with scaled simulations of sodium jet discharge following postulated pipe rupture accidents, to provide more realistic descriptions of sodium dispersal patterns, sodium drop size, and sodium drop energy transfer. An initial model of sodium drop energy transfer (SODROP)[6,7] has been developed, and shows fair agreement with tests conducted to date. These models will permit proper engineering assessment of the design pressure requirements of LMFBR primary cells. The characteristics of SODROP, in terms of functions, input requirements, and design data output, are listed in Table 2.

TABLE 2

SODROP CHARACTERISTICS

Functions	Input Requirements	Design Data Output
Sodium Droplet - Gas Heat Transfer Rate	Peroxide-Monoxide Ratio, 0 to 1	Cell and Containment Design Pressure
Sodium Droplet Burning Rate	Fraction of Total Volume Swept by Droplets	Dynamic Loading Factor of Structure
Oxygen Consumption (initial oxygen from 21 to 0%)	Droplet Size Distribution	Oxygen Consumption
Temperature of Gas and Walls		Sodium Consumed — Sodium Remaining
Cell Pressure Rise		Aerosol Source for HAA-3
Sodium Consumption		
Sodium Droplet Temperature		

C. HAA-3 (Aerosol Transport Behavior)

The aerosol behavior model, HAA-3,[8,9] is currently utilized to provide the source term for leakage of sodium oxide, radioactive fission products, and PuO_2 from LMFBR-FFTF outer containment for site radiological dose analysis, based on certain hypothetical accidents. These calculations then form the basis for the design leak rate of the containment building. The HAA-3 model provides a description of the natural aerosol depletion mechanisms, such as agglomeration and growth of initially sub-micron size particles and fallout of the agglomerates, as well as transport of the aerosol between inner and outer containment barriers. Radiological source term analyses conducted prior to the development of aerosol

agglomeration models did not take into account these aerosol depletion mechanisms, resulting in unrealistic overestimates of site radioactivity for hypothetical accidents. The HAA-3 model has been initially verified with sodium oxide aerosols in a 30-ft tall test chamber. Additional testing of the model with UO_2 aerosols (as a simulant for PuO_2), as well as mixed aerosols of UO_2 and sodium oxide, is currently in progress. The characteristics of HAA-3, in terms of functions, input requirements, and design data output, are listed in Table 3.

TABLE 3

HAA-3 CHARACTERISTICS

Functions	Input Requirements	Design Data Output
Aerosol Particle Size Distribution – Suspended	Oxide Release Fraction of Burned Sodium vs Time (pool or sodium droplet)as Source Term	Input for Site Dose Calculation
Aerosol Suspended Concentration	Initial Particle Size – Log Normal	Filter Loading
Aerosol Agglomeration (Brownian-gravitational)	Gravitational Agglomeration Efficiency	Plated Aerosol Fraction
Aerosol Settled	Stokes Settling Correction Factor	Settled Aerosol Fraction
Aerosol Plated	Wall Plating (concentration gradient distance)	Particle Size for Filter Design or Lung Retention
Aerosol Ventilated	Leakage of Aerosol Equivalent to That of Gas	
	Fission Product Release Fraction	

D. SOFAACS – System Utilization

The utilization of the three codes which comprise SOFAACS for LMFBR accident analysis applications is carried out by employing the basic functions of each of the individual codes with appropriate input data, in a particular operational sequence and using required interfacing procedures and information. The SOFAACS codes, SOFIRE II, HAA-3, and SODROP, are not chained together to generate calculations for a given application in one continuous computer run. However, the output from any one of the codes is easily converted to input for one of the others. The basic utilization of SOFAACS codes for generating design data for various LMFBR engineered safeguards applications is shown in Figure 1. A more detailed summary of code interfacing and input requirements for specific accident applications is presented in the next section.

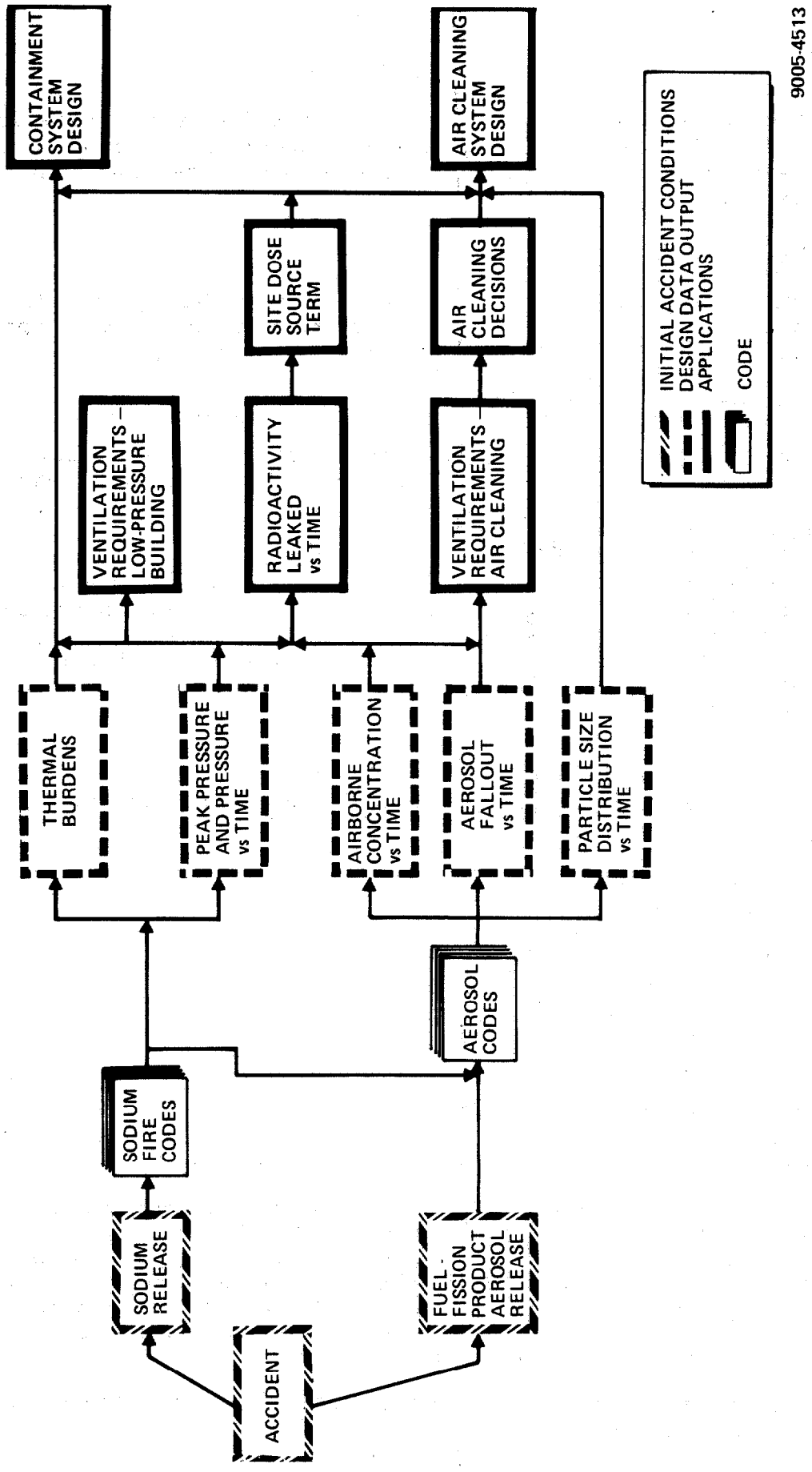

Figure 1. SOFAACS – Basic System Utilization

III. SOFAACS Applications

The operating sequences, interfaces, and input requirements for specific applications of SOFAACS are shown in system flow sheets for postulated accidents involving sodium release, and fuel and fission product release from the primary heat transfer system.

A. Sodium Release

Figure 2 shows the applications flow sheet for large sodium pool spills and fires, and for dispersed sodium releases such as are postulated in the Hypothetical Core Disruptive Accident (HCDA) or a pipe rupture accident.

B. Fuel and Fission Product Release from Primary System

The applications flow sheet for fuel and fission product release from the HCDA and a large pool fire containing contaminated sodium is shown in Figure 3.

C. Typical System Application

An example of a typical application of SOFAACS is presented in Figure 2 for the sodium release cases of a large pool spill. The spill is postulated to occur in a primary system cell which is open to the containment building during system maintenance. The initial conditions for the spill and systems configuration are presented in Table 4.

TABLE 4

INITIAL CONDITIONS – LARGE POOL SPILL

Cell Volume (ft^3) = 2.63×10^4
Spill Area in Cell (ft^2) = 2.3×10^3
Building Volume (ft^3) = 1.3×10^6
Sodium Spill Temperature (°F) = 350
Diameter of Open Access Port (ft) = 10
Weight of Sodium Spill (lb) = 167,000
Oxygen Concentration (%) = 21
Building Design Leakage (%/day at 2 psi) = 0.3
Sodium Oxide Release Fraction = 0.3

The first set of calculations obtained in the operating sequence for this application is shown in Figure 4, and are the output from the SOFIRE II 2-cell code calculation. These output data are then used as input to the next step in the process – computing aerosol transport HAA-3 code. Design data output from the HAA-3 calculation is shown in Figures 5 and 6. With appropriate input information to HAA-3, this particular example can also be used for evaluating the air cleaning aspects of this postulated accident.

Table 5 summarizes input data requirements for the several codes and notes current status.

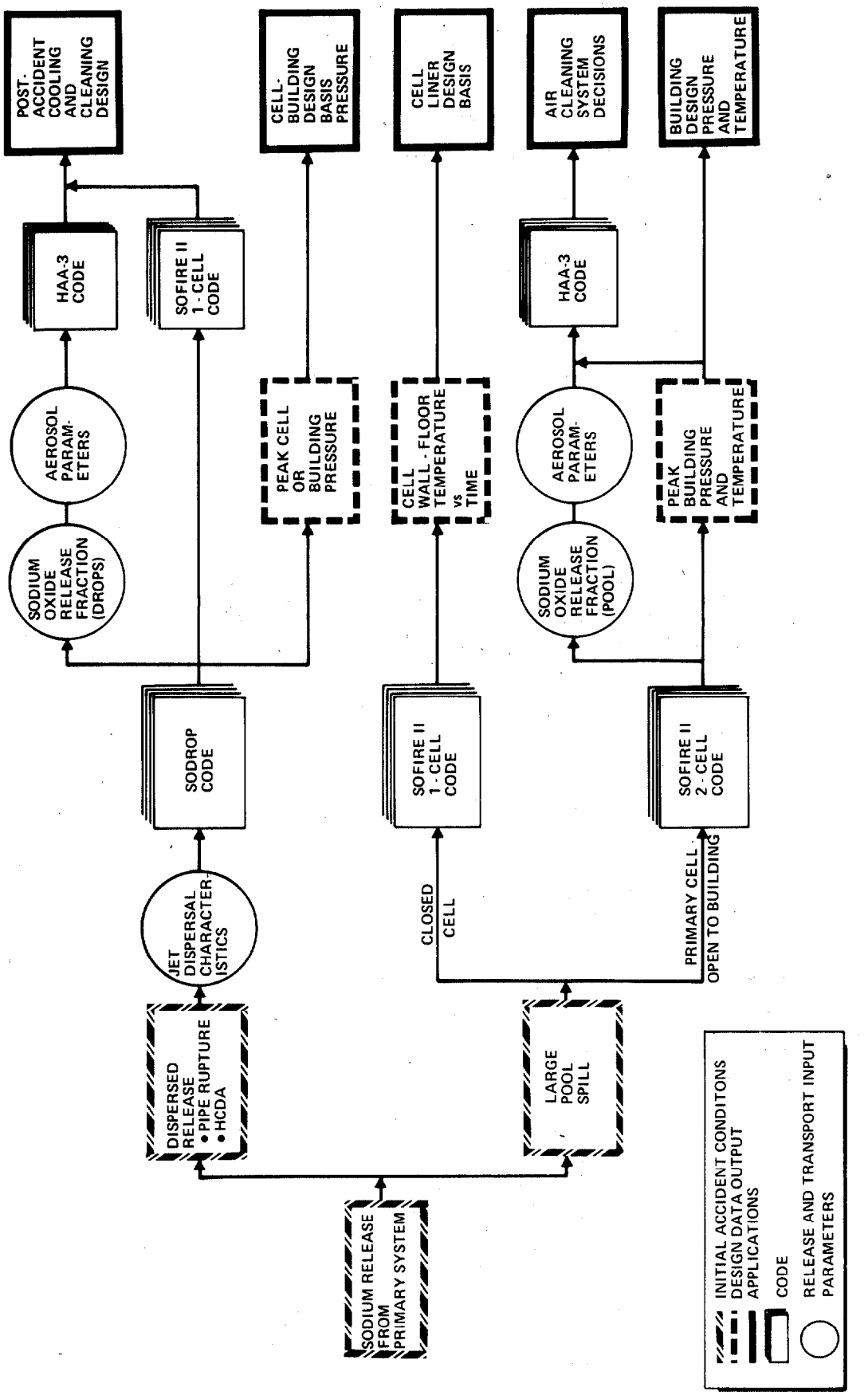

Figure 2. SOAFAACS – Sodium Release Applications

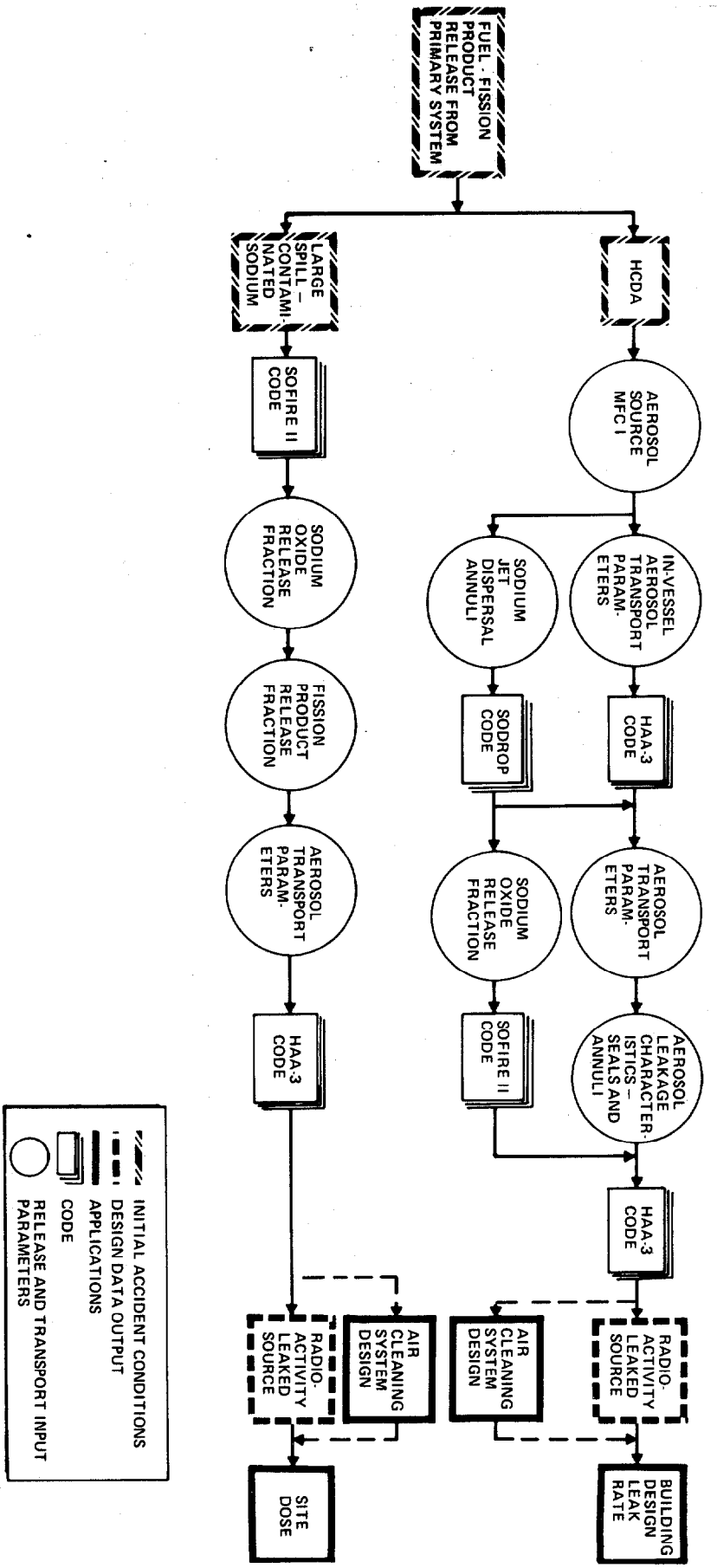

Figure 3. SOFAACS – Fuel and Fission Product Release Applications

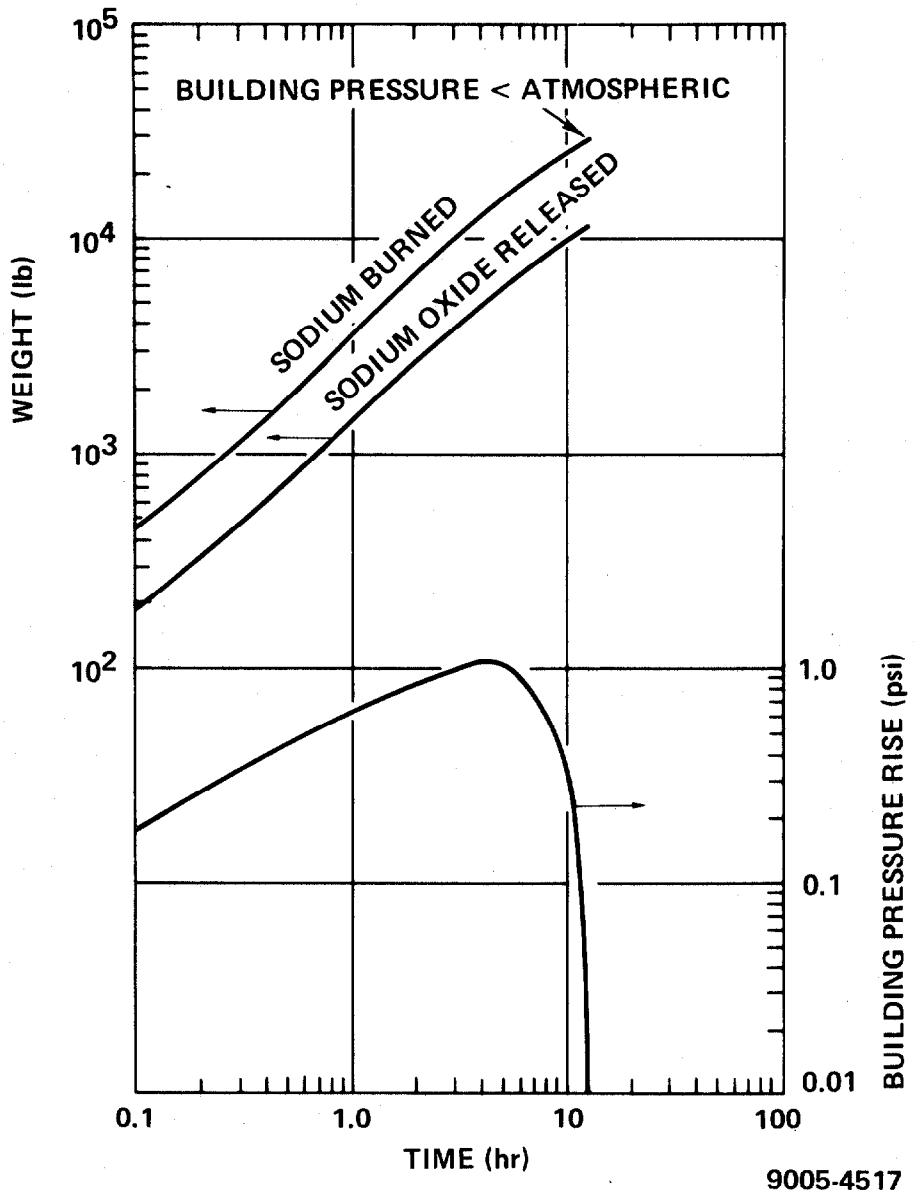

Figure 4. Sodium Pool Fire – Primary Cell Open to Containment Building (SOFIRE II 2-cell computations)

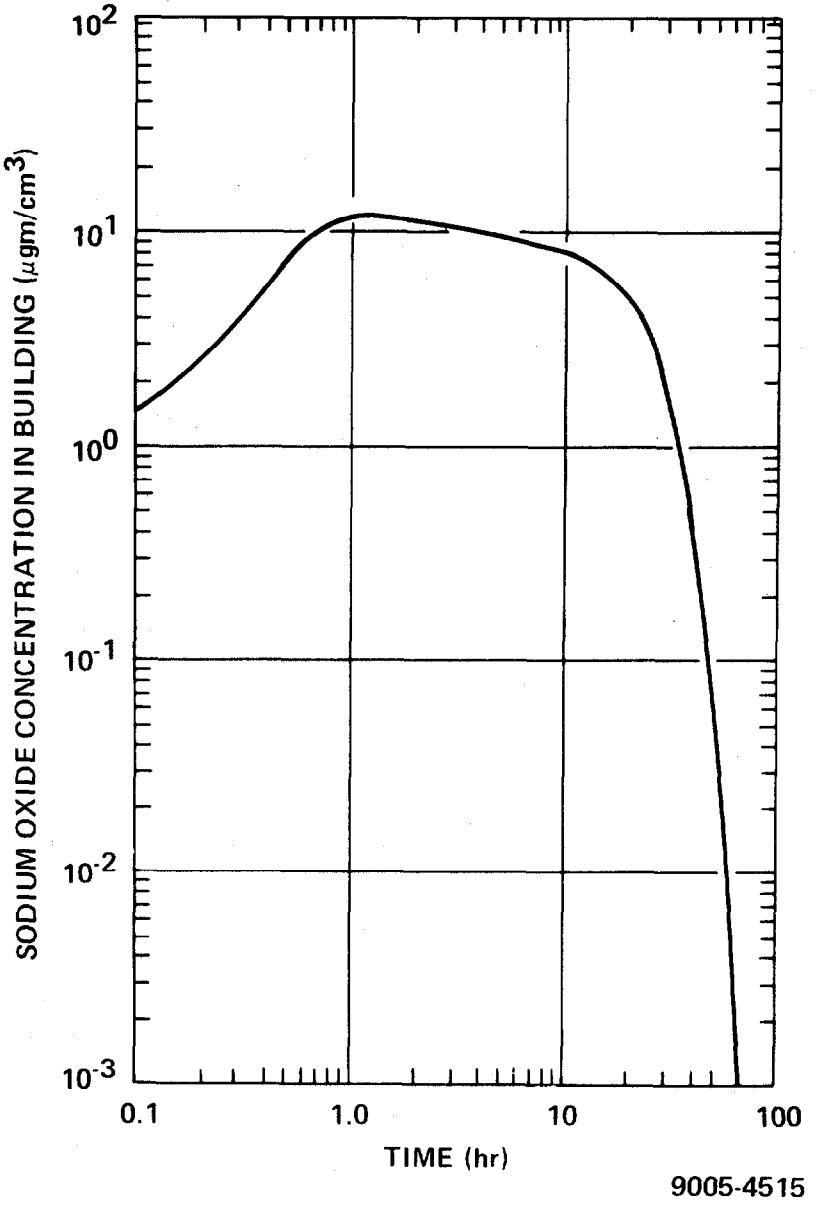

Figure 5. Sodium Pool Fire—Primary Cell Open to Containment Building (HAA-3 computations)

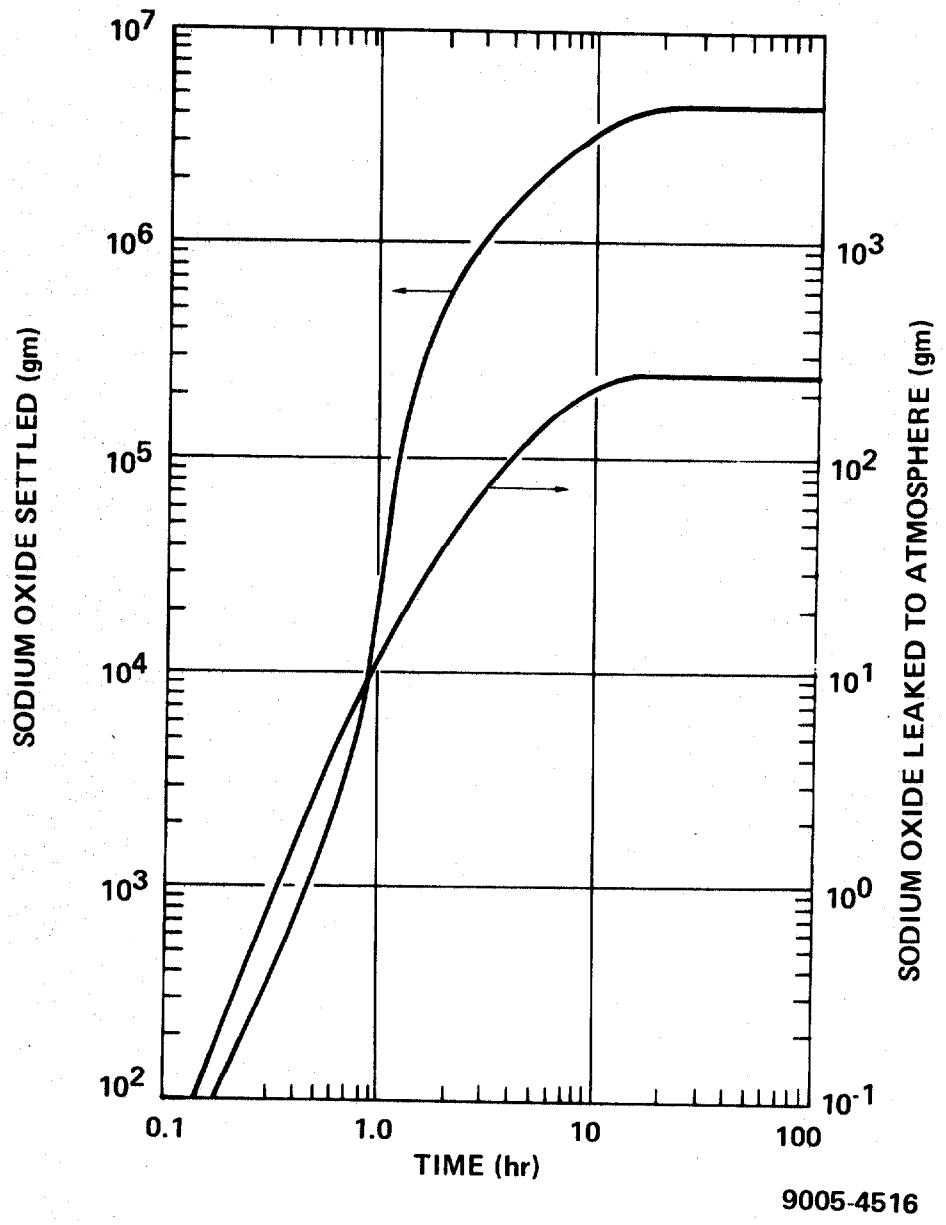

Figure 6. Sodium Pool Fire – Primary Cell Open to Containment Building (HAA-3 computations)

References

1. Proceedings of the Ninth AEC Air Cleaning Conference, Boston, Mass., September 1966; CONF-660904, Vol. I and II (December 1966)
2. Proceedings of Symposium on Treatment of Airborne Radioactive Wastes, New York, August 1968; IAEA, Vienna (1968)
3. Proceedings of the Tenth AEC Air Cleaning Conference, New York, N. Y., August 1968; CONF-680821 (December 1968)
4. Proceedings of the Eleventh AEC Air Cleaning Conference, Richland, Washington, September 1970; CONF-700816, Vol. I and II (December 1970)
5. "SOFIRE II User Report," Atomics International (to be published)
6. Atomics International, "Annual Technical Progress Report, LMFBR Safety Programs, GFY 1971," AI-AEC-13006 (September 15, 1971)
7. Atomics International, "Quarterly Technical Progress Report, LMFBR Safety Programs, October-December 1971," AI-AEC-13020 (February 15, 1971)
8. R. S. Hubner, "An Approximate Solution to the General Equation for the Coagulation of Heterogeneous Aerosols," AI-AEC-Memo-12880 (1969)
9. R. S. Hubner, E. U. Vaughan, and L. Baurmash, "HAA-3 User Report," Atomics International, AI-AEC-13038 (to be published)

INPUT DATA REQUIREMENTS AND STATUS

CODE	PARAMETER	STATUS
SOFIRE II	COMBUSTION PRODUCT RATIO (Na_2O_2/Na_2O)	TEST DATA
SODROP	COMBUSTION PRODUCT RATIO	TEST DATA
	VOLUME SWEPT BY DISPERSAL	PRELIMINARY TEST DATA
	DROPLET SIZE DISTRIBUTION	PRELIMINARY TEST DATA
HAA-3	SODIUM OXIDE RELEASE FRACTION FROM BURNING	TEST DATA
	INITIAL PARTICLE SIZE – LOG NORMAL	TEST DATA
	GRAVITATIONAL AGGLOMERATION EFFICIENCY	TEST DATA FOR SODIUM OXIDE, URANIUM OXIDE IN 30-ft VESSEL – HIGH CONCENTRATION URANIUM OXIDE AND MIXTURES NEEDED
	STOKES SETTLING CORRECTION FACTOR	
	WALL PLATING (CONCENTRATION GRADIENT, DISTANCE)	TEST DATA
	LEAKAGE OF AEROSOLS THROUGH CONTAINMENT LEAK PATHS	EQUIVALENT TO A GAS – REALISTIC DATA NEEDED
	FISSION PRODUCT RELEASE FRACTION FROM BURNING	TEST DATA, IODINE ONLY – DATA FOR OTHERS NEEDED

Table 5

DISCUSSION

FIRST: The output of these programs which you have described certainly represent a short-cut to evaluating the consequences of an accidental release. What would you estimate to be the reliability of the output in terms of standard error or any other way of measuring the confidence level that you have in these numbers?

SILBERBERG: That's a very good question. Now that we are integrating the various aspects of the program we have started to look at this question very hard. I will not quote a number at this time, but that number would be a function of the various uncertainties in the input parameters which I have mentioned. What we are proceeding to do now, is to put limits on the uncertainties in the input data, cycle them through the system, and to determine the envelope of these uncertainties on the entire progression of an accident. One can then get a good feeling of what is the optimistic side and the pessimistic side. We have run experiments and compared them with the individual codes. For example, just recently we started to test the two-cell version of Sofire-II. For those tests that we have run to date in the program, we find that we are getting fairly good agreement between code and experiment, and when I say "fairly good", I mean much better than, say, 50 percent. In the case of aerosols, based on the conditions that we've tested, which are a good representation of inner containment situations, we feel that the reliability of the code is good. If anything, we feel we are conservative in terms of safety considerations; particularly because of the assumption of leakage of aerosols through containment as a gas.

PARTICLE DEPOSITION AND REENTRAINMENT ON FFTF H&V COMPONENTS FOLLOWING A SODIUM SPILL

M. W. First, E. Jochem,
T. W. Baldwin, R. Hall
Harvard School of Public Health
665 Huntington Avenue
Boston, Massachusetts 02115

Abstract

The purpose of sodium aerosol deposition tests underway at HACL is to examine basic sodium deposition mechanisms in heat-exchanger tubes which simulate as closely as possible the tube size, flow rates, and aerosol characteristics under consideration for the FFTF. On the basis of test data, it should become possible to predict total sodium deposition from a knowledge of particle size and concentration, flow rate, and duration for any accident condition (whether currently under study or of future interest) and make possible a prediction of the effect this is likely to have on heat transfer capability. The experiments currently conducted at HACL do not and are not intended to simulate accident conditions for the purposes of investigating "source terms" or the manner in which molten sodium vaporizes, nucleates, and cools under accident conditions.

I. Introduction

Closed loop cells in the FFTF contain major sodium recirculation equipment and must be cooled to protect the machinery enclosed in the space from over-heating. Plans call for the atmosphere inside the cell (0.5-2.0% oxygen, the remainder nitrogen) to be recirculated continuously through an externally-located heat exchanger by a centrifugal or axial flow fan. Because leakage of molten sodium from the equipment inside the closed loop cell will generate sodium oxide aerosols and, when the sodium spill is of sufficient magnitude to consume all available oxygen in the sealed space, metallic sodium aerosols, the system must be protected from excessive deposition of aerosol particles in the heat exchanger and blower if the cooling function is to be maintained during and after a spill.

Sodium aerosol filters located upstream of fan and cooler were considered to be a satisfactory method of preventing sodium deposition in these pieces of equipment (1,2), but space limitations in a redesigned FFTF containment housing made filters impractical. Therefore, studies were undertaken to examine critically the amount of deposition which would be likely on heat exchanger surfaces following a sodium spill of moderate size and to design, if possible, sufficient excess heat exchanger capacity to overcome the loss in efficiency caused by the fouling of the surfaces. Deposition experiments have been conducted with finned-tube and with shell-and-tube heat exchangers, and the experimental results correlated with particle deposition theory.

II. Experimental Results

A. Deposition in a Finned-tube Coil.

Figure 1 shows the arrangement of apparatus inside the aerosol chamber that was used to test an 8-row deep finned-tube coil. The blower is capable of moving 1400 cfm against a resistance of 4 in.w.g. The test tunnel was provided with a flow measuring orifice meter, temperature probes, pressure taps to measure filter resistance, and a flow regulating damper. Sodium samplers were installed up and downstream of the filter. Face velocity was 500 fpm. Coolant was not used during this experiment so all surfaces were at the same temperature as the aerosol. Oxygen concentration was 1% during this test, and airborne sodium concentrations ranged between 0.3 and 1 gram/m^3.

The pressure drop across the 8-row coil at constant air flow rate was monitored as an index of particle deposition. During the first 150 minutes of steady flow at 500 cfm, the pressure drop increased from 0.145 to 0.155, a rise of 0.01 in.w.g. During the next 67 minutes, pressure drop rose to 2.7 in.w.g., indicating a more rapid rate of particle deposition which produced a progressive narrowing of the flow channels in the coil. During the next 8 minutes of operation, the pressure drop rose to 3.8 in.w.g. and the flow rate fell from 500 to 260 cfm. At 500 cfm (had the blower been capable of this flow at this resistance) the coil resistance would have been approximately 14 in.w.g. This behavior is shown graphically in Figure 2. An initial period of slow resistance increase was followed by a period of rapid rise, and, finally, nearly complete blocking of the flow channels. This may be seen in Figure 3, a photograph of the cooling coil section after deposition of sodium. If the experiment had continued, total blockage of these channels by deposited sodium aerosol particles would have occurred. This behavior can be explained by reference to the mechanisms responsible for particle deposition. The largest weight fraction of the particles (i.e., > 80%) is above 0.5 μm and therefore inertial deposition is the principal separating force. As the air passages in the coil become smaller by deposition of particles, velocity for the same volumetric flow rate increases and inertial separation, highly dependent on velocity, increases also. Thus, an accelerating rate of deposition accounts for an accelerating rate of pressure drop increase. This suggests that operation at normal face velocities, i.e., 1000 to 1500 fpm, will result in more efficient particle deposition.

During the 225 minutes that the coil was exposed to a flow rate of 500 cfm, there was a total deposition of 44 grams of sodium. The average concentration of sodium in the aerosol during this period was 0.69 grams/m^3 (toward the end of the period the sodium reservoir became depleted and the airborne concentration declined). This means that approximately 3000 grams of sodium passed through the coil during the experiment and that approximately 1.4% was retained in the coil. This is a small amount compared to the total coil volume, but as the photograph in Figure 3 indicates, deposition occurred principally on the upstream face of the coil and eventually formed a

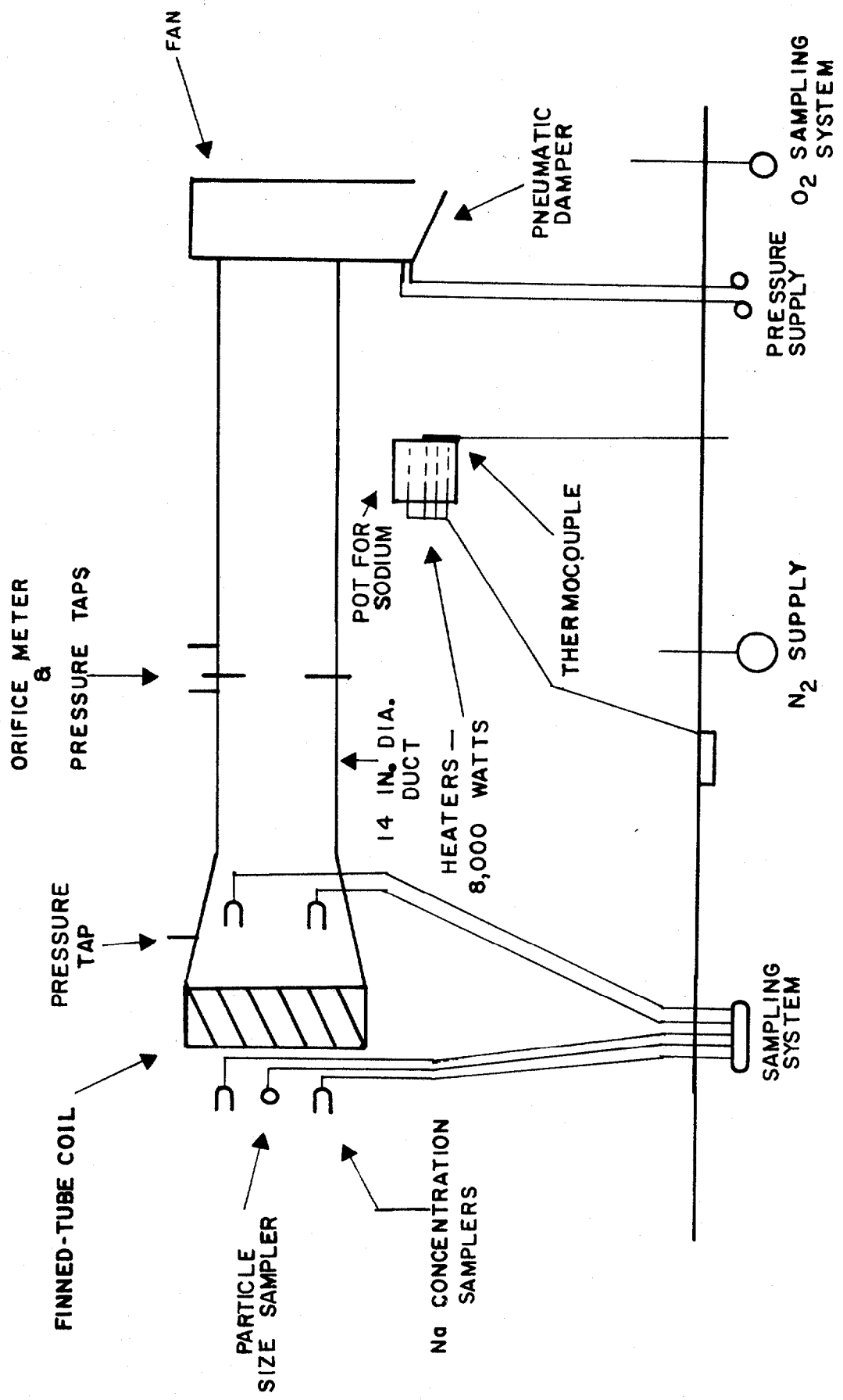

FIGURE 1

Arrangement of apparatus for deposition tests.

FIGURE 2

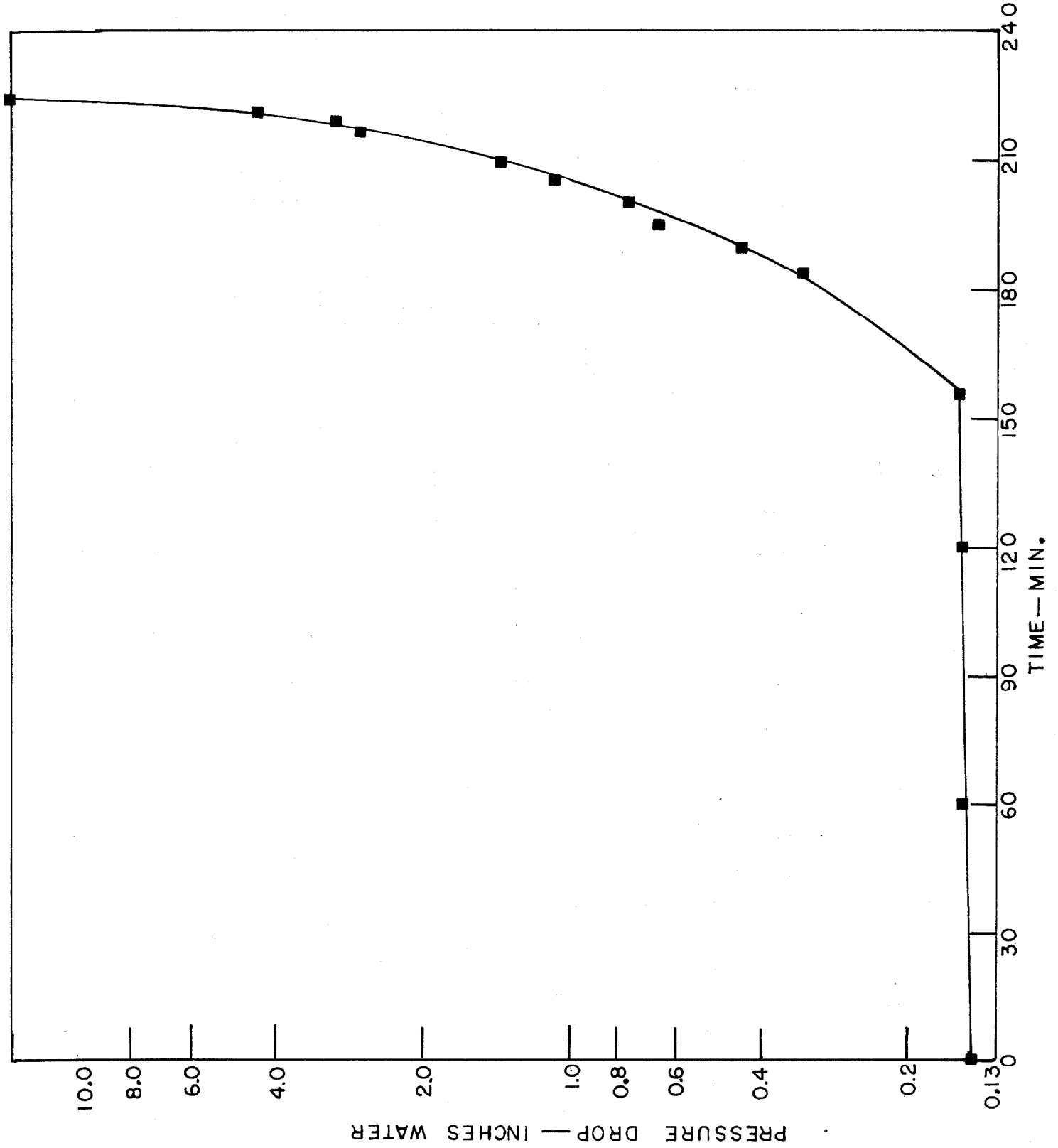

Cooling coil air flow resistance as sodium particles deposit between fins.

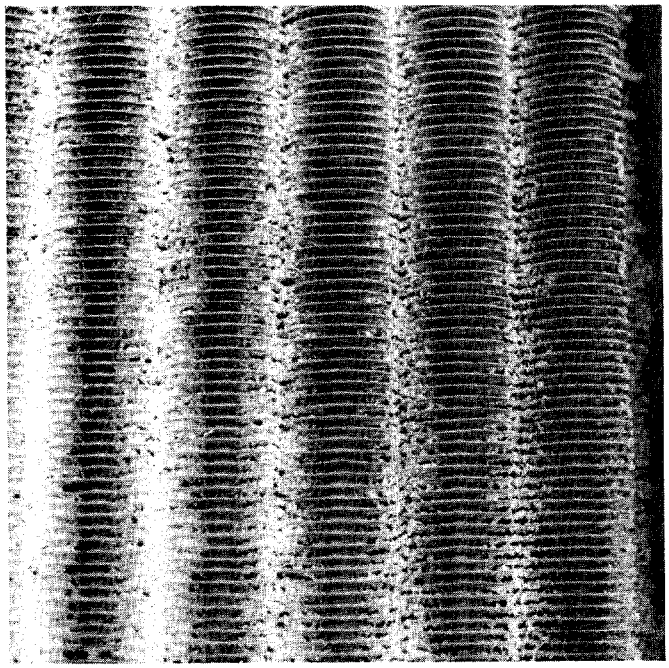

Figure 3. Face of finned cooling coil showing sodium deposits.

substantial obstruction to flow.

B. Deposition in Tube-type Heat Exchangers

The above studies, combined with other considerations, resulted in design changes in the closed loop cell cooling system. A shell and tube heat exchanger with coolant in the shell was substituted for the finned-tube cooler. The proposed shell-and-tube cooler contains 2600 0.56-inch I.D. gas flow tubes, each 8-ft. long. A 3-tube assembly of 0.53-in. I.D. tubes, 8-ft. long, was constructed as a heat exchanger simulator for sodium aerosol deposition studies. Figure 4 shows the experimental arrangement. Aerosol was withdrawn from the chamber, passed through the tubes at the design flow rate of 90 fps, and blown back into the chamber through a second wall port. Sodium deposition was monitored by continuously observing the increase in the pressure drop of the tubes at constant volumetric flow rate (i.e., as the tube openings became narrowed by deposition, tube velocity increased). However, as the experiment progressed, the maximum static pressure capability of the recirculating blower was reached and from that time onward, when the experiment was continued, volumetric flow rate declined at constant pressure drop across the tubes. Clean tubes at design flow rate have a pressure drop of 11.4 in.w.g. Maximum measured pressure drop after deposition was 21.1 in.w.g.

Table 1 summarizes three test series. In each case, the chamber was totally filled with a sodium cloud before starting the recirculating blower that induced flow through the heat exchange tubes. For test number 1, two pounds of sodium were evaporated into the chamber gas in about 50 minutes. This produced very high particle concentrations (up to 6.8 grams, as Na, per cubic meter) and vigorous agglomeration. Visible suspended particles (> 100μm) were produced. Gas volume rate began to decline after 21 minutes and the experiment was terminated after 50 minutes. Figure 5 shows the tube inlet at the conclusion of the test (with an unused tube bundle for comparison) and Figure 6 shows the outlet. Figure 5 shows inlet deposition of sodium to form a pyramidal inlet contour but the tubes are open to almost their full diameter. This is shown more clearly in Figure 7 which is the inlet end after the deposit on the tube sheet had been carefully removed (again with a clean tube for comparison). Figure 8 is a similar photograph of the outlet end. (Please note that prior to the photograph we disturbed the sodium deposit in attempting to measure its thickness). In both cases, the deposit on the tube walls is obvious. At the inlet end, it was about 0.05 in. thick; at the outlet, about 0.02 in. Thirty grams of sodium (as Na) were recovered from the interior of the three tubes after removal of the surface deposits on the inlet and outlet tube sheets.

Tests 2 and 3 were conducted with aerosols containing about one order of magnitude less particle loading. For test number 2, the run was halted after 69 minutes when the blower was no longer able to maintain the design gas flow rate. Total deposit in the tubes was 17.6 grams, as Na. Test number 3 was run 228 minutes. Again, it was possible to maintain rated flow for 69 minutes; but after that, flow declined steadily until, at the end, it was only 18% of the design value and pressure drop across the tubes was 21.1 in.w.g. at this low

Figure 4. Experimental arrangement for studies of sodium deposition in 0.53-in. tubes.

1. Sodium aerosol chamber
2. Inlet pipe
3. Cascade impactor
4. Thermocouple
5. Tube bundle
6. Oxygen monitor
7. Flow meter
8. Valve
9. Recirculating blower
10. Chamber gas drier
11. Cooler tube pressure taps
12. Pressure drop monometer
13. Set of replacement tubes

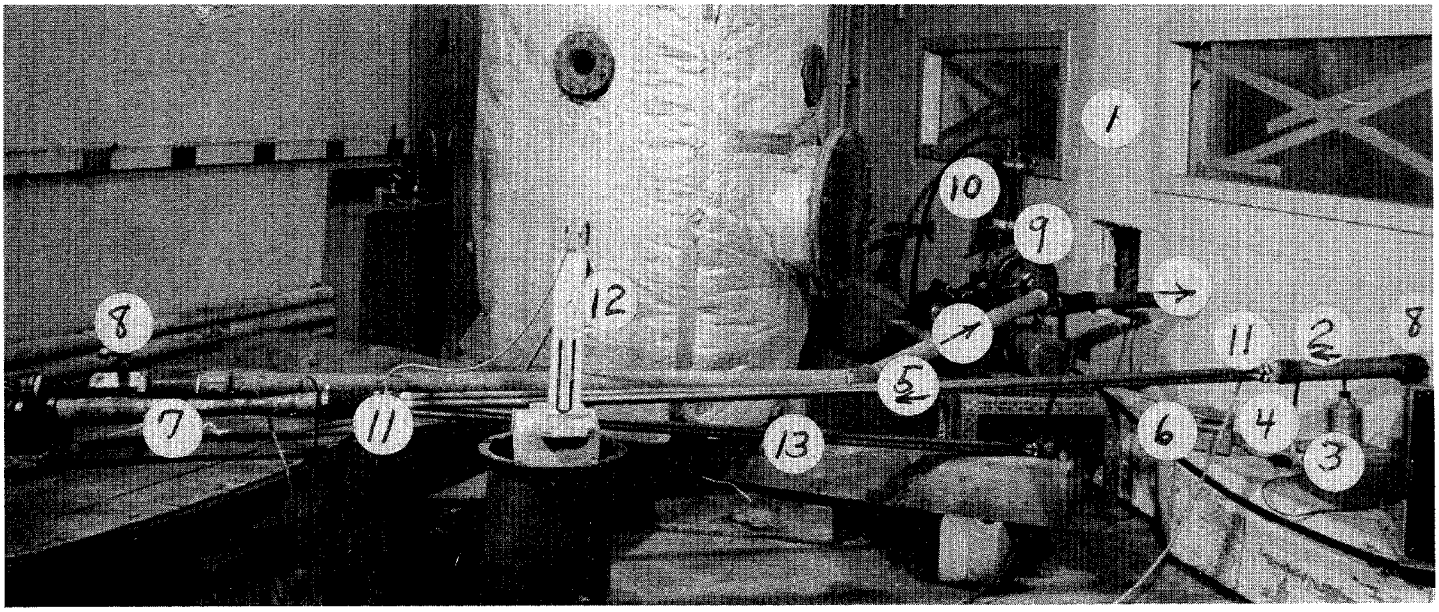

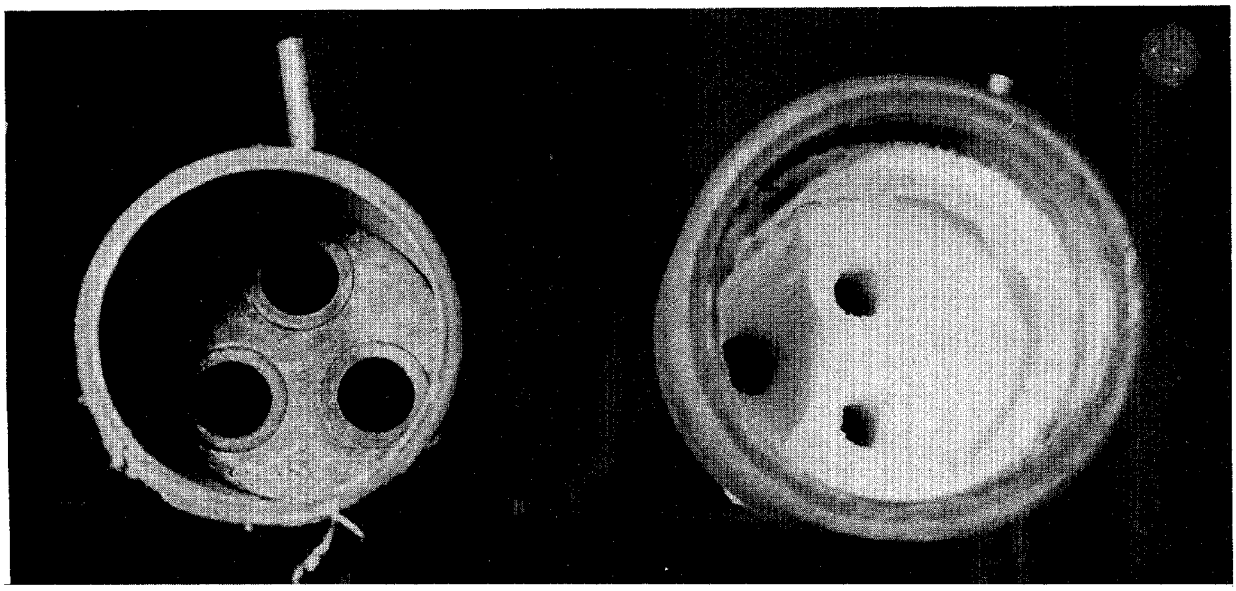

Figure 5. Entry tube sheet before and after sodium deposition

TABLE I

SODIUM DEPOSITION IN 0.53-in. I.D. HEAT EXCHANGER TUBES

	Test #1 1/13/72	Test #2 1/18/72	Test #3 1/21/72
Loading - gm/M^3			
Maximum	6.8	0.90	1.12
Minimum	.26	0.24	0.21
Average	4.4	0.48	0.72
Running Time - Min.	71	69	228
Total Deposit in Tubes - gm Na	30	17.6	32
Velocity ft/sec.	92 for first 21 min.	90	90 for first 69 min.
	92-81 over last 50 min.		90-16 over last 159 min.
Temperature °F			
Outside tube	77	73	75
Inside tube	95	85-89	90
Pressure Drop in. of water			
Maximum	18.0	20.3	21.1
O_2 - %			
Before test	1.4	1.1	1.2
After test	1.1	1.1	--
Water vapor lb. water/lb. N_2			
Before test	0.00146	0.0009	--
After test	0.00088	0.00029	--

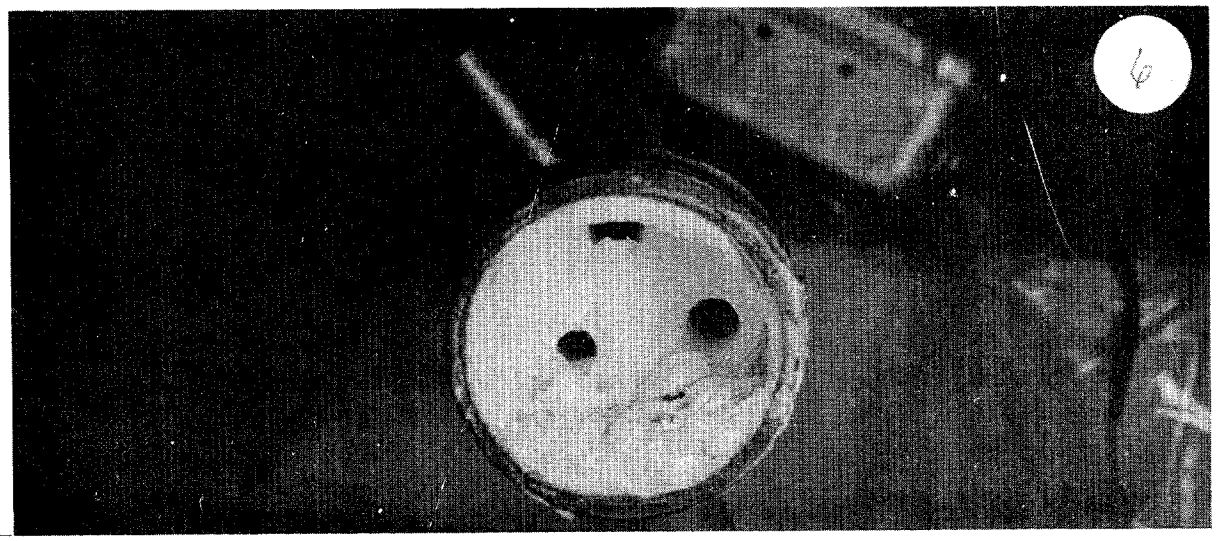

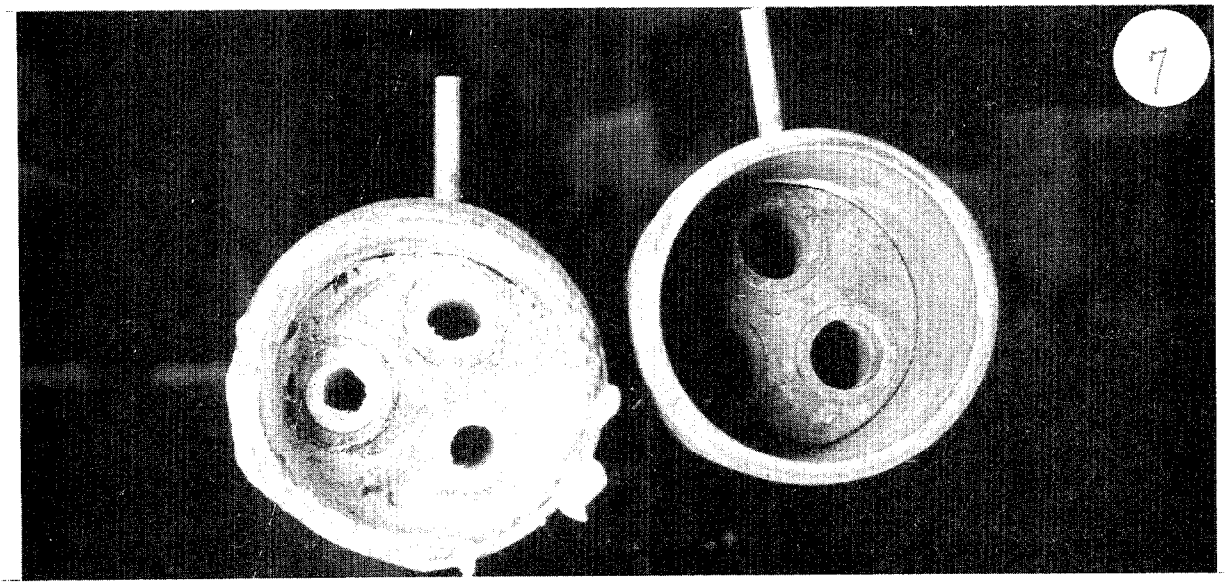

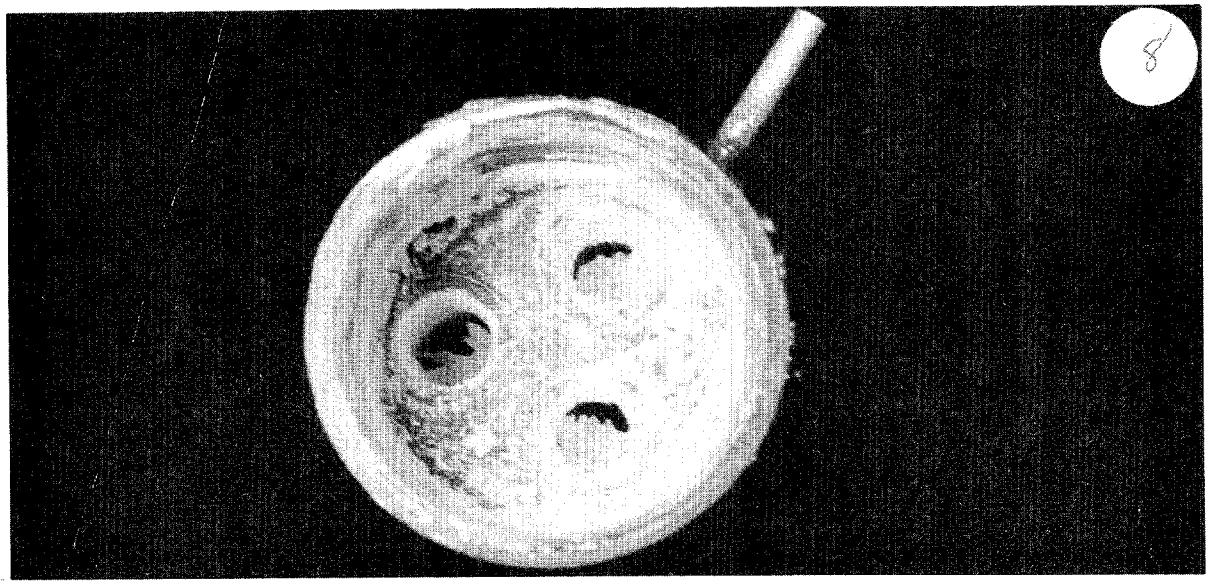

Figure 6. Exit tube sheet after sodium deposition
Figure 7. Inlet tubes after removal of tube sheet deposit
Figure 8. Outlet tubes after removal of tube sheet deposit

flow rate. Figure 9 shows the inlet tube sheet at the conclusion of test number 3. It is obvious that the tubes are almost totally closed off. Figure 10 shows the entry tube sheet after the deposit at the entry had been removed. Again, it is clear that the deposit has almost completely plugged the tubes. Probings with a stiff wire indicated that the thick wall deposit extended 12 to 14 inches into the tube. Figure 11 shows the exit end of the tubes after the deposit on the tube sheet had been removed.

It is clear from these three tests that substantial wall deposition may be expected in 0.56 I.D. tubes at a tube velocity of 90 fps when the tubes are not protected by entry filters.

It is possible to deduce from the data in Table 1 that particle deposition occurs at a rate that is proportional to the sodium concentration in the aerosol and the time of operation. Other factors, such as gas temperature and particle size, shape, and specific gravity are important as well, but by generating the test aerosol as uniformly as possible and as closely similar to the predicted source term as possible, particle concentration and time of exposure remain as the principal deposition variables in the current series of experiments.

C. Deposition in a Centrifugal Recirculating Blower

It was proposed that blowers on closed loop cell cooling systems be placed upstream of the heat exchanger to remove some of the particulate sodium before it reaches the exchanger tubes. Therefore, two runs were conducted with the recirculation blower upstream of the heat exchanger tubes. In the first, conducted for 87 minutes, sodium aerosol concentrations averaged 0.08 gm/m^3. This is about one order of magnitude less than aerosol concentrations of previous experiments and total deposition in the heat exchanger tubes was approximately one order of magnitude less, indicating the direct relationship between aerosol concentration and mass deposition rate in grams per minutes. During this period, only 1.8 grams of sodium (as Na) deposited in the tubes and airflow resistance increased 1.5 in.w.g. but a total of 29 grams of sodium (as Na) deposited in the blower casing. In the second run, conducted for 140 minutes, the sodium aerosol concentration entering the blower was 1 gm/m^3. Design flow rate, equivalent to 90 fps through the tubes, began to decline after 70 minutes and reached a low of 33 fps before the run was terminated. Tube deposition over the 140 min. exposure period totaled only 2.7 gm. This is approximately proportional to 1.8 grams deposited in 87 minutes during the previous run and demonstrates the proportionality of deposition with time of exposure for equal aerosol concentration flowing through the tubes. However, 54 grams (as Na) had deposited in the blower casing and almost completely plugged it with solid sodium oxide as shown in Figure 12a, the blower outlet, and Figure 12b, the blower inlet. Details of the two runs are summarized in Table 2.

From these two runs, it is evident that placing the recirculation blower upstream of the heat exchanger will, indeed, reduce the deposition load on the heat exchanger but only at the risk of rapid blower failure by sodium deposition in the blower passages.

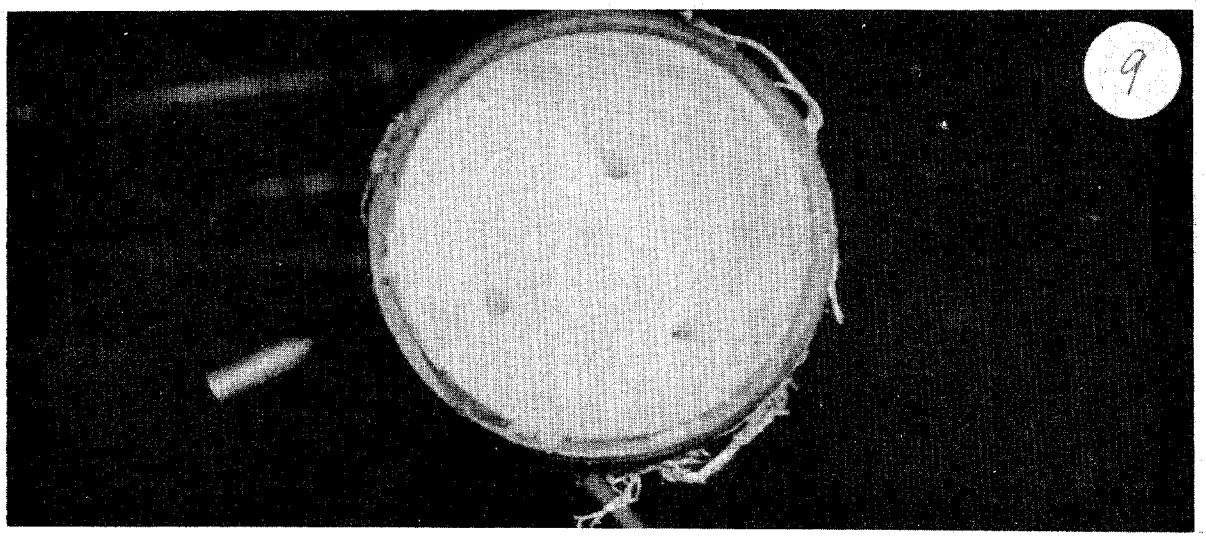

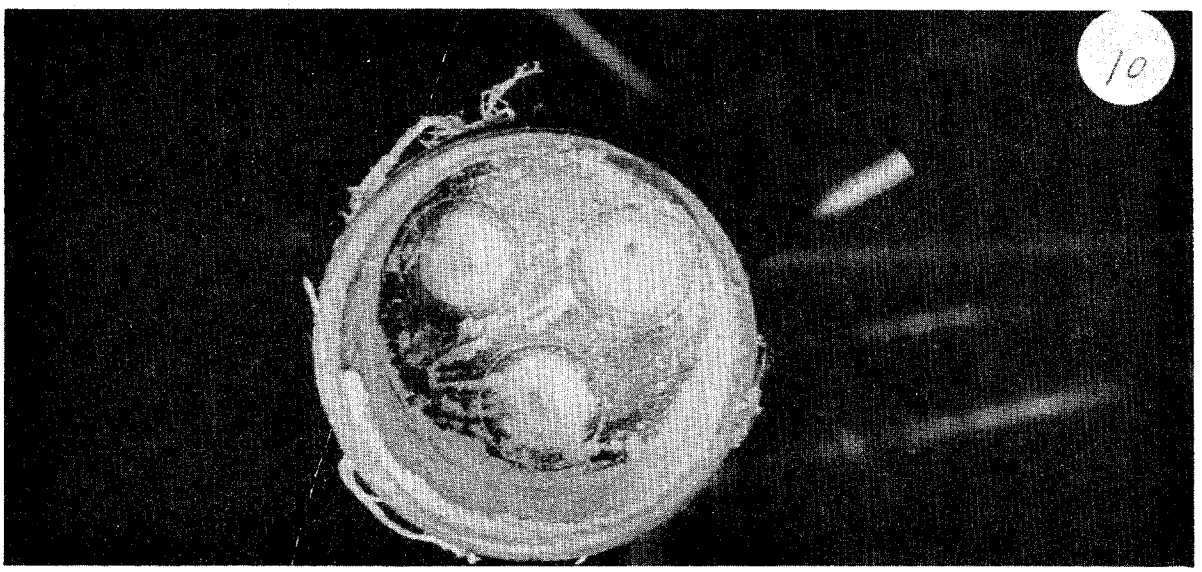

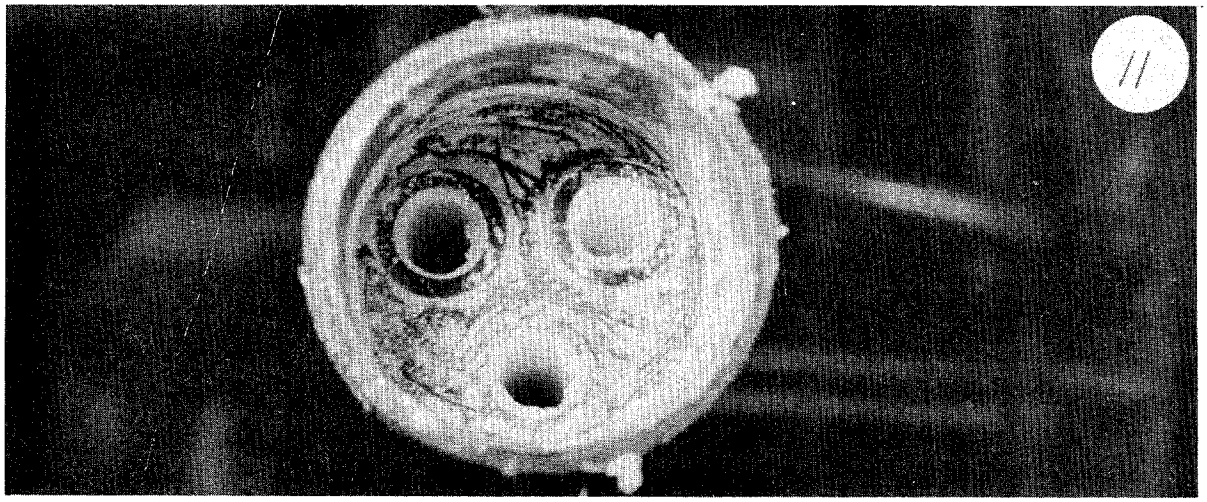

Figure 9. Inlet tube sheet at end of test 3.
Figure 10. Inlet tube sheet at end of test 3 after removal of entry deposit.
Figure 11. Outlet tube sheet at end of test 3 after removal of exit deposit.

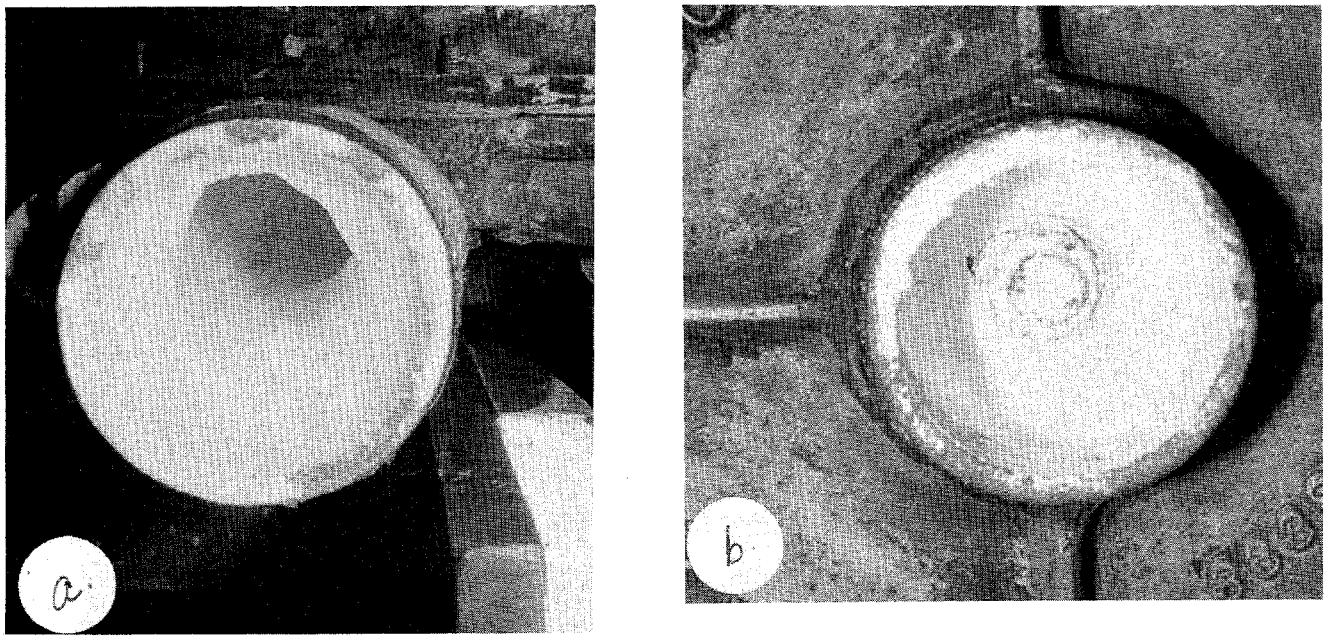

Figure 12. Recirculation blower upstream of heat exchanger tubes after 140 min. exposure to 1 gm/m^3 sodium oxide aerosol. a. outlet; b. inlet.

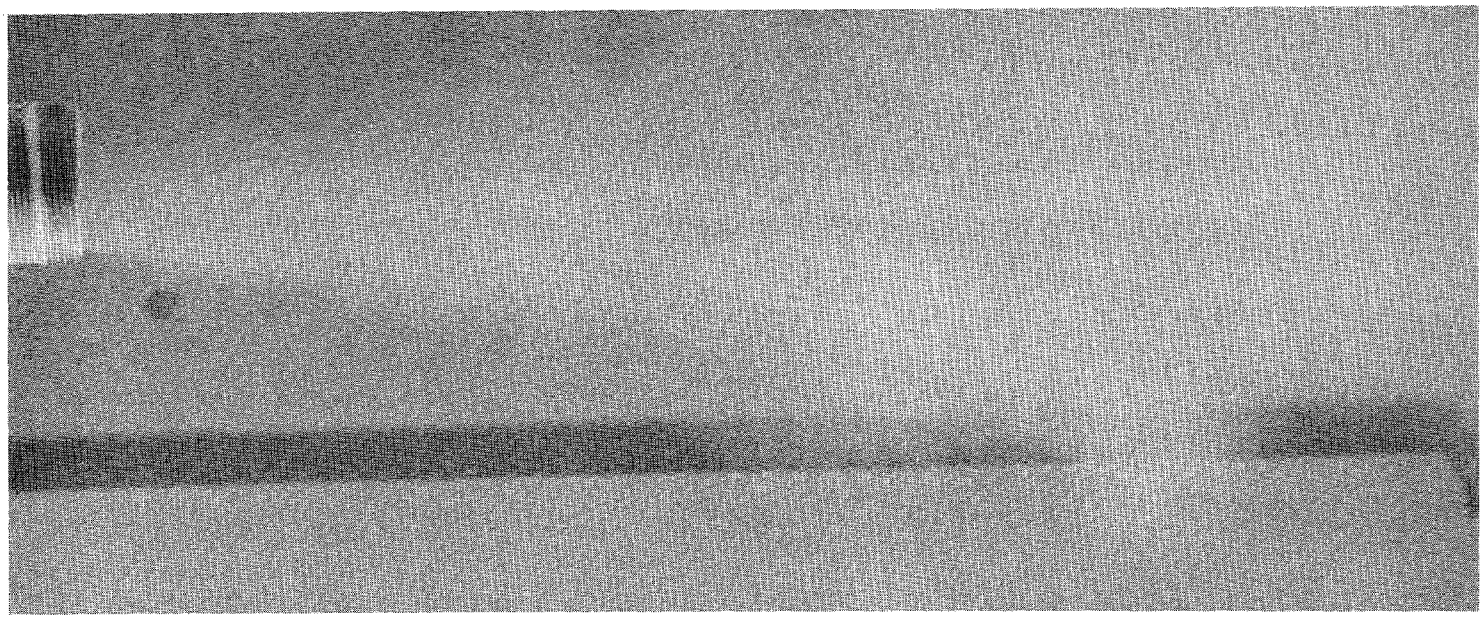

Figure 13. Cleaning caked dust from heat exchanger tube with compressed nitrogen pulse (calcium carbonate).

TABLE 2

TWO DEPOSITION RUNS WITH RECIRCULATING BLOWER UPSTREAM OF HEAT EXCHANGER TUBES

	1/28/72 Test #1	2/8/72 Test #2
Loading at tube entrance ($gm\ Na/M^3$)		
Maximum	0.10	0.28
Minimum	0.033	0.06
Average	0.08	0.16
Loading at fan entrance ($gm\ Na/M^3$)		
Average	--	1-2
Running time - min.	87	143
Total deposit in tubes (gm Na)	1.8 (2.5) calc.	2.7
Total deposit in blower (gm Na)	29	55
Tube velocity-ft/sec.	90	90 for first 70 min. 90 to 50 for last 73 min.
Temperature °F		
Outside tube	75	75
Inside tube	102	104
Pressure drop in. of water		
Maximum	12.9	(4.5 at end)
O_2-%		
Before test	1.3	1.9
After test	1.1	--
Water vapor (lb. water/lb. N_2)		
Before test	.0009	.00014
After test	--	--

From previous experiments, it is clear that with the blower downstream of the tubes, failure of the heat exchanger may occur from excessive deposition if the aerosol concentration reaching it is abnormally high or aerosol flow is abnormally prolonged. Therefore, methods of removing sodium deposits from heat exchanger tubes while the unit is in normal operation were investigated as an alternative to filtration.

D. Tube Cleaning during Normal Service

Tube cleaning tests were conducted first in normal air using finely ground calcium carbonate as a sodium oxide simulant. It was found that short (1-sec) bursts of compressed nitrogen (150 psi) introduced at the exit end of the tube and directed upstream were effective in removing deposited dust. Figure 13 shows dust being discharged from a tube during a simulation test. Next, similar static tests were conducted with tubes in which freshly formed sodium oxide had deposited by standard exposure methods described previously. Tubes were cleaned with one, two, and four successive one-second compressed nitrogen blasts. The expelled sodium was collected in filter bags and the residual sodium washed out. Both fractions were analyzed for total sodium and gave the following results:

Cleaning cycles of 1-sec at 125 psi	Amount Na blown out of tube (gm)	Amount Na remaining in tube (gm)	Total Na deposited (gm)
1	0.94	4.6	5.7
2	2.2	3.5	5.6
4	3.8	0.9	4.7

Next, dynamic cleaning tests were conducted using one-second compressed nitrogen blasts each time the heat exchanger tubes reached an elevated airflow resistance signifying excessive sodium oxide deposition. The three compressed nitrogen jet tubes installed in the discharge header of the experimental heat exchanger tube bundle are shown in Figure 14a. Figures 14b and 14c show the inlet and outlet ends of the heat exchanger tubes at the conclusion of a multicycle run during which the pressure drop through the tubes (and hence the thickness of the sodium coating which affects heat exchange rate) had been well controlled by occasional nitrogen blasts. The nitrogen jet tubes shown in Figure 14a had been removed prior to recording Figure 14b. These tubes were centered on the tube axes and mounted approximately 0.1 inch back of the tube end. Figure 15 shows the compressed nitrogen cylinder, pressure reduction valves, pulse timer, and external attachments to the blast cleaning tubes. Table 2 summarizes the details of two runs using repeated dynamic tube cleaning gas blasts during continuous operation. It was found that 150 psi pressure was not adequate for satisfactory tube cleaning under dynamic conditions and the pressure was raised to 250 psi. Total nitrogen released during a 1-second blast at 150 psi was 6.4 liters; at 250 psi, 13.6 liters; both at NTP. Two runs of approximately

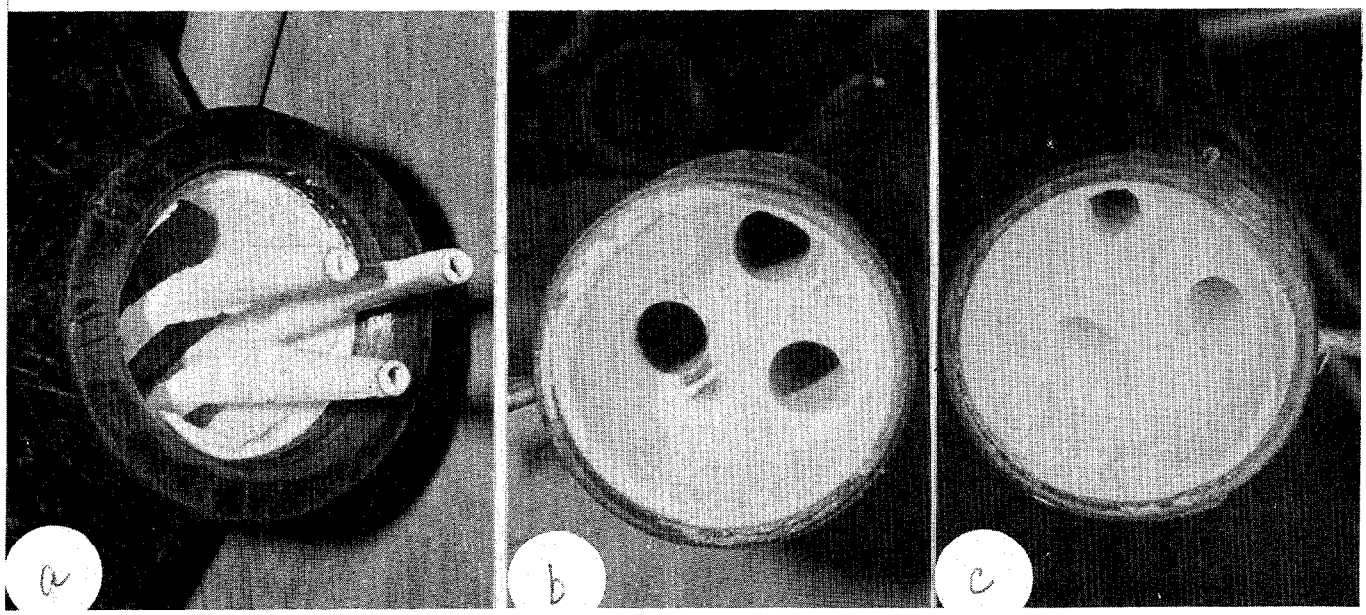

Figure 14 a. Nitrogen jets at downstream end of heat exchanger tube bundle.
b. Discharge end of tube bundle
c. Entry end of tube bundle.

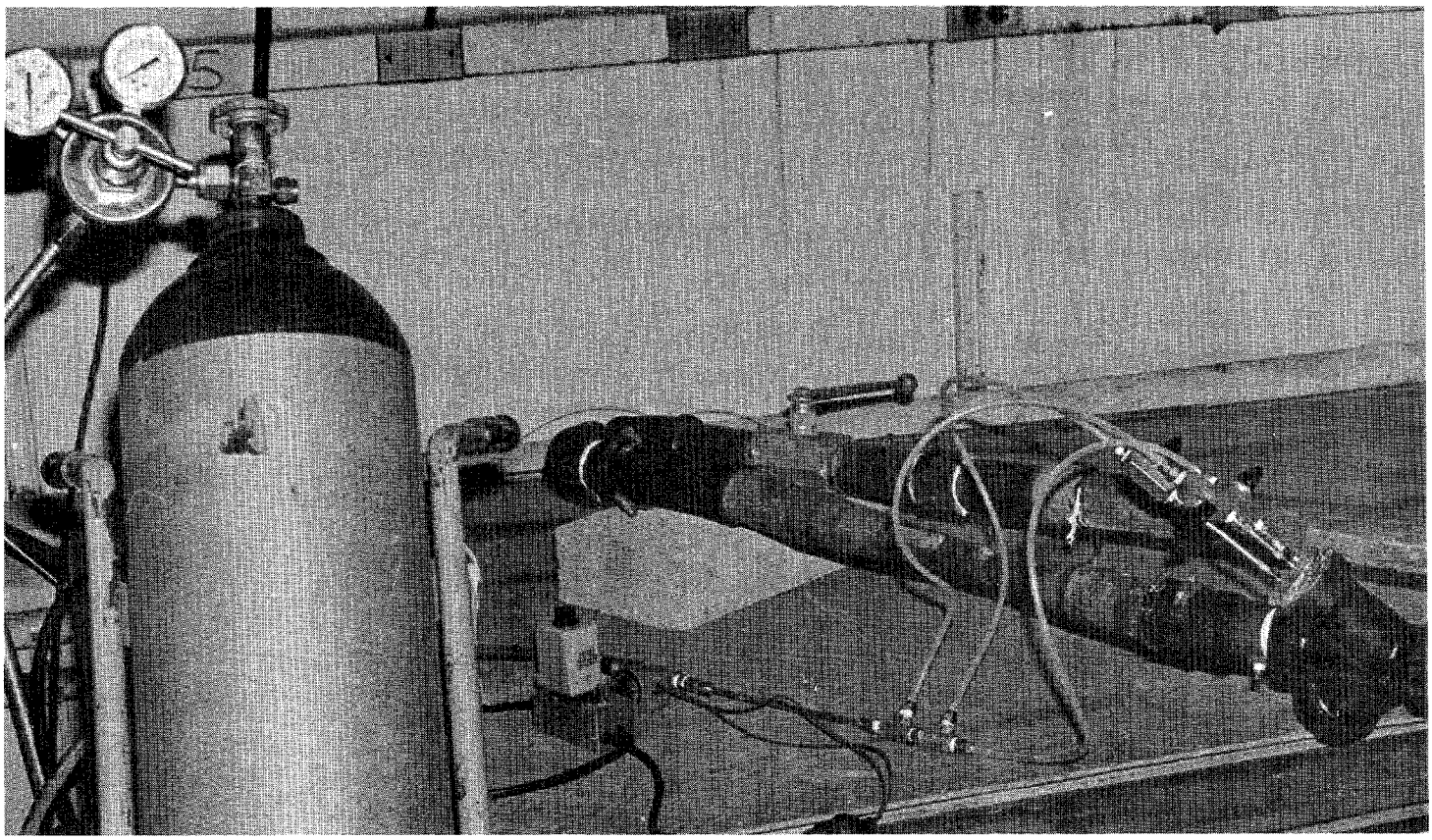

Figure 15. Jet tubes attached to compressed nitrogen cylinder, showing jet pulse timer and pressure reduction valves.

200 minutes were conducted at sodium concentrations averaging 1.3 and 4.2 grams/m^3 without significant rise in tube resistance. After each of the 8 cleaning cycles of Run 2 in Table 3, tube resistance was lowered to a value close to clean starting resistance and it seemed probably that this run could have carried on indefinitely with similar results. Lower nitrogen gas pressures (and less total nitrogen consumption) would be equally effective if the recirculating blower could be shut down for a few minutes during the cleaning process.

III. Deposition Theory

Neither the phenomenon of turbulent particle deposition on surfaces nor particle reentrainment due to the action of turbulent motions of the carrying stream has yet been fully developed. A review of recent deposition theories and experimental studies (and, also, of the less well understood subject of particle reentrainment) suggests accuracies, at best, to within about one order of magnitude; and, often, much less than this. The various theories which have been proposed lack agreement among themselves. This is caused, in part, by (1) differing assumptions and simplications introduced into the various models (2) disagreement about the correct experimental methods to be used to verify the models and (3) differences in particle generation; errors in sizing, flow, and concentration measurements; and undetected reentrainment.

For all deposition models, the deposition surface has been assumed to be a perfect sink and only monodisperse aerosols plus radial inertial and diffusive removal mechanisms have been considered. In addition, many authors have assumed that the eddy diffusion coefficient of fluid momentum transfer and the eddy diffusion coefficient of material transfer are equal. From all indications, this assumption seems to be an oversimplification. Often, an assumption is made that particle transport from the bulk fluid to the region next to the walls is very rapid with respect to particle transport to the wall and particle deposition is deduced to take place by a 'free flight' mechanism whereby the particle traverses the final boundary layer in projectile fashion. All these models differ, however, in their prediction of the starting point of the particle's free flight and its velocity. Sehmel (3) tested by statistical methods four models published by others plus one of his own against results calculated from experimental deposition velocities. These statistical tests showed that the five models did not adequately represent the experimental data.

A review of different experimental investigations shows that some authors have omitted information necessary for data comparison, e.g., many times, such important parameters as geometric standard deviation of the particle size distribution, agglomeration rate, surface stickiness and roughness, thermophoretic and electrostatic effects, and inlet and outlet effects are not mentioned. Therefore, it is difficult to evaluate the different models by reference to experimental results.

Despite a data scatter of one order of magnitude, two empirical equations derived by Sehmel from the experiments of four workers

seem to give the most satisfactory results in predicting turbulent deposition.

(1) $K = 1.47 \cdot 10^{-6} \cdot \rho_p^{1.01} \cdot d_*^{2.1} \cdot \left(\frac{D \cdot \bar{U}}{\nu}\right)^{3.02} \cdot \left(\frac{f}{2}\right)^{0.5} \cdot \bar{U}$ for perfect sinks

(2) $K = 1.10^{-17} \cdot \rho_p^{1.83} \cdot d_*^{2.99} \left(\frac{D \cdot \bar{U}}{\nu}\right)^{3.08} \cdot \left(\frac{f}{2}\right)^{0.5} \cdot \bar{U}$ for perfect and non-perfect sinks

where

K = deposition velocity

ρ_p = density of particles

d_* = ratio of particle diameter in μm to duct diameter in cm

D = duct diameter

$\bar{U}$ = average flow velocity

ν = kinematic viscosity

f = friction factor

There is no adequate theory to account for reentrainment. Those that have been proposed predict no reentrainment for particles $\leq$ 20μm under conditions where entrainment has been observed experimentally; and particles as small as 2μm can be removed by turbulent reentrainment (4). A kinetic model cannot be applied because of a lack of knowledge of the particle removal velocity profile within the laminar sublayer. Experimental results are confusing as it is possible to maintain a certain rate of reentrainment despite greater deposition due to increasing Reynolds number or particle size. In addition, there appear to be no data available on friction forces of deposited layers which would permit prediction of reentrainment by breaking up and sloughing off of whole chunks of deposit. Thus, there is little reliable information available for application to the practical problem of reentrainment at the present time. Nonetheless, the best available information has been applied to the specific problem of deposition and reentrainment of sodium aerosols in turbulent flow while passing through a shell-and-tube heat exchanger. It is estimated that the design equations will give results accurate to within one order of magnitude.

When comparing predicted results by deposition models with experimental observations, the decrease in tube diameter caused by the deposition layer has not been considered. This may be part of the reason why some calculated values of deposition velocity, K_{cal}, underpredict measured deposition velocities, K_{exp}, since, for constant flow rates, Reynolds Number, average flow velocity, $\bar{U}$, and the diameter ratio, d_*, increase with decreasing tube opening. Therefore, a mean diameter, D_m, was defined to calculate deposition velocity for a three tube assembly of 1.346 cm. I.D. tubes. Assuming

a linear increase in thickness of the deposition layer from inlet to outlet, the mean flow channel diameter at the half distance through the tube, L/2, and at the half time during which deposition takes place, $\Delta t/2$, may be calculated as follows:

$$\frac{\pi}{4}(D^2-D_m^2) = \frac{\pi}{4}(D_m^2-D_{1/2}^2)$$

where

$$D_{1/2} = \frac{D_i+D_o}{2}$$

Final tube diameter at the inlet end, D_i, and at the outlet end, D_o, were determined by analyzing photographs of inlet and outlet, (i.e., D_i = 0.99 cm; D_o = 1.07 cm) following a deposition run. The experimental deposition velocity is calculated from:

$$K_{exp} = \frac{m_{exp}}{n_t \cdot (\pi \cdot D_m \cdot L) \cdot C_{av} \cdot \Delta t}$$

where m_{exp} is the total mass deposited and C_{av} is the average aerosol concentration during deposition.

The average density of the depositing sodium aerosol, ρ, is taken as the bulk density of Na_2O. Comparing predicted and experimental values of deposition velocity, a close agreement may be noted in Table 3. For test number 2, deposition was calculated two ways; first, for the initial conditions of a completely open tube diameter, i.e., $D_m = D$, and uniform flow velocity, $\bar{U}$; and second, for average conditions with constant volumetric gas flow rate.

The design equations require additional runs for verification over a wider range of conditions. Accurate results require accurate determination of the mass median diameter, MMD, of the depositing particles and of the deposition layer at each end of the tube. In our deposition studies, we found deposit density, ρ, to be about 0.17 g/cm^3. The experiment did not permit measurement of reentrainment, but there is evidence that reentrainment did not occur during these tests, i.e., using Sehmel's relationship for reentrainment, the critical distance, y_d^+, is less than 0.5 in all cases (see Table 3) and the good agreement between experimental and calculated deposition was obtained by using design equation 1 and assuming no reentrainment.

Table 3 - Recent Sodium Studies

Test No.	ρ g/cm^3	MMD μm	σ_g	$\bar{U}$ $\frac{cm}{sec}$	D_m cm	ν $\frac{cm}{sec}$	K_{exp} $\frac{cm}{sec}$	K_{cal} $\frac{cm}{sec}$	$\frac{K_{exp}}{K_{cal}}$	m_{exp} g	m_{cal} g	C_{av} g/cm^3	Δt sec	y_d^+
2	0.57	4.12	1.6	2740	1.346	0.1682	3.57	1.76	2.03	17.6	9.73	0.43	4140	0.382
2	0.57	4.12	1.6	2740	1.21	0.1682	3.57	3.74	.095	17.6	18.54	0.43	4140	0.426
4	0.57	4.12	1.6	2740	1.346	0.1682	**1.30**	1.76	0.74	1.8	2.30	0.08	5220	0.382

References

1. Viles, F. J., Jr., Himot, P., and First, M. W., High Cap -- High Efficiency Filters for Sodium Aerosols, Harvard Air Cleaning Laboratory, Boston, Massachusetts Report # NYO-841-10 (August, 1967).

2. M. W. First, T. Baldwin, "Sodium Aerosol Filtration Studies", Proceedings of the 11th AEC Air Cleaning Conference, Richland, Washington (31 August-3 September 1970), p. 445.

3. Sehmel, G. A., "Particle Deposition from Turbulent Air Flow", Journal of Geophysical Research, Vol. 75, No. 9, pp. 1766-1781 (March 20, 1970).

4. Sehmel, G. A. "Complexities of Particle Deposition and Re-entrainment in Turbulent Pipe Flow", Aerosol Science, Vol. 2, pp. 63-72 (1971).

5. First, M. W., et.al. Semiannual Progress Report,#NYO-841-20, Harvard Air Cleaning Laboratory, Boston, Massachusetts (October, 1969).

The research reported in this paper was supported by an Air and Gas Cleaning Contract of the U.S. Atomic Energy Commission under Contract Number AT(11-1)3049 with Harvard University.

DISCUSSION

MURROW: Three questions. First, what happens to the deposit when you use the reverse jet effect, where does it go, and do you recommend a place for it to go? Second, you had several heat exchangers in series, how many would be required before the last one would not become clogged? Third, would the reverse jet effect be appropriate for the fin type exchanger?

FIRST: You are quite right in surmising that there must be a chamber at the end of the heat exchanger tubes to receive the material that is blown out. This material is highly agglomerated and I don't believe it will take a settling chamber of any great size to collect it. Our settling chamber was quite modest in dimensions and we had no difficulty. I doubt that heat exchangers in series is a practical solution to deposition. You may recall that I gave a figure of 1.4 percent as the amount deposited from the aerosol flowing through the finned-coil heater. If only one or two percent deposits from the flowing aerosol, it is going to take a lot of heat exchanges in series before the concentration falls to a low value. We did not try blowing back the finned-coil heat exchanger. I think this might have worked; although there is so much open area that the jet might spread too much to be effective.

ZAVADOSKI: Do you expect that increased temperatures caused by a lack of heat removal will enhance deposition or retard it?

FIRST: The theoretical analysis takes into account deposition by thermophoretic forces. It turns out that thermophoresis will not produce much effect for particles larger than a few tenths of a micrometer. As the weight of material represented by particles less than 0.5 μm is probably less than 20 percent, the total effect will not be serious one way or the other. In other words, one could neglect this factor, although it is a very important one for small particles, and still not be far off on the estimate of total deposition.

ZAVADOSKI: Do you expect to run heated tests or test a heat exchanger under actual operating conditons?

FIRST: The former. We are scheduled to receive a mock-up of the final design capable of handling 1,400 CFM that we can test under design operating conditons.

FISH, J: What was the cooling fluid that you were using? Presumably it wasn't water.

FIRST: I should have mentioned that these were isothermal experiments, i.e., coils with no coolant.

FISH, J: Then it was simply deposition. As there was no coolant flowing through the coil, you didn't get the temperature gradient you would experience in a real coil?

FIRST: This is right and, in line with the question asked a moment ago about the effect of temperature differences, I believe that temperature effects should be investigated, but we haven't gotten to it yet; we expect to shortly. We performed one experiment in which we tried to determine the heat transfer coefficient. To magnify the temperature difference, we elected to use ice water on the outside of the tube. Although our moisture content inside the test chamber was very low, our experiment was destroyed because we did, indeed, get moisture pickup by the sodium oxide inside the tube. There are a number of important effects we haven't investigated yet.

FISHER, B: What is the chemical constitution of this sodium oxide? Is there an appreciable percentage as peroxide?

FIRST: In our experiments we are working with atmospheres below two % O_2; and below one % in most of our experiments. Na_2O_2 represents less than 5 percent of the total oxide; it is almost all monoxide. We anticipate that as elemental sodium evaporation continues, and as the oxygen content of our test chamber declines to zero, we will go through a phase where we will have a mixture of sodium monoxide and metallic sodium. Eventually, when all the oxygen has been consumed, we will get to the point where we will be generating an aerosol of pure sodium metal.

SILBERBERG: I might add that we observed similar results. At low oxygen concentrations, i.e., up to two percent, the composition of the oxide is essentially all monoxide, Na_2O. As you approach 5 percent oxygen environments, and on up to normal air, you produce appreciable quantities of peroxide.

To summarize the session, I think there were several important points that evolved. One, that in LMFBR accident considerations we are dealing with potentially large quantities of sodium aerosols which can influence air cleaning applications rather seriously. We, therefore, must be able, not only to predict sodium aerosol behavior for design, but we must also learn to cope with the effects of possible sodium releases. Today, in Dr. First's paper, we heard one example of information relating to the handling of such situations.